



ORIGINAL ARTICLE

Experimental and computational phase behavior investigation for the CO₂ + 1H, 1H-perfluorooctyl acrylate and CO₂ + 1H, 1H-perfluorooctyl methacrylate systems at high pressure



Duraisami Dhamodharan¹, Min-Soo Park¹, Suhail Mubarak, Hun-Soo Byun^{*}

Department of Chemical and Biomolecular Engineering, Chonnam National University, Yeosu, Jeonnam 59625, South Korea

Received 17 January 2023; accepted 23 March 2023

Available online 30 March 2023

KEYWORDS

High-pressure phase behavior;
Carbon dioxide;
PFOA;
PFOMA

Abstract The solubility information of fluoro-monomer (meth) acrylate in organic solvents is an important factor affecting their use in numerous engineering practices. This study investigated the phase equilibria of 1H, 1H-perfluorooctyl acrylate (PFOA) and 1H, 1H-perfluorooctyl methacrylate (PFOMA) in supercritical CO₂ using optical fiber and contact lenses. The solubility curves investigations were conducted at different temperatures (313.2 to 393.2) K and pressures (3.31 to 16.84) MPa, and the mole fraction of (0.032 to 0.630). Results revealed that the PFOA + S_C-CO₂ and PFOMA + S_C-CO₂ systems exhibited a type-I behavior. The RMSD (%) for the PFOA + S_C-CO₂ [k_{ij} = 0.075, η_{ij} = 0.0], and PFOMA + S_C-CO₂ [k_{ij} = 0.075, η_{ij} = 0.0] models using two factors determined at 353.2 K evaluated with the alterable parameters at each T were 5.08 %, and 5.36 %, respectively. The correlation of the experimental response for the PFOA + S_C-CO₂ and PFOMA + S_C-CO₂ two component models were examined using Peng-Robinson (PR) equation of state (EOS) involving two parameters (k_{ij}, η_{ij}) base on a fluid mixture rule. Additionally, the critical properties (p_c, T_c and ω) and vapor pressure of PFOA and PFOMA were assessed using the Joback-Lydersen group impact.

© 2023 The Author(s). Published by Elsevier B.V. on behalf of King Saud University. This is an open access article under the CC BY-NC-ND license (<http://creativecommons.org/licenses/by-nc-nd/4.0/>).

1. Introduction

Currently, the use and development of polymers, particularly in engineering application, such as coating sources, biomedical resources, aircraft materials, optics, and fibers, have increased. Fluoropolymers have demonstrated attractive and exceptional characteristic behaviors such as superior thermal stability, water resistance and high chemical stability. Particularly, polymers with lengthy fluoro-functional chains have attracted significant interest. The polymers with acrylate and (meth) acrylate repetition group (i.e., monomer) are primarily utilized

^{*} Corresponding author.

E-mail address: hsbyun@jnu.ac.kr (H.-S. Byun).

¹ The first and second authors contributed equally.

Peer review under responsibility of King Saud University.



Nomenclature

Symbols

a Pa·m⁶/mol² Attraction factor
 b m³/mol

Co-volume factor

BP MPa Bubble point

CP Critical point

DP Dew point

N Number of the data

p MPa Pressure
 R 8.314462 J/(mol·K) Universal gas constant
 T K Temperature
 v m³ mol⁻¹ Molar volume
 x Liquid phase mole fractions

Greek letters

α Alpha function
 ω Acentric factor

in a variety of functions which are in medicine, glazing, oil additives, toy industry and building materials (Kirk-Othmer, 1981). Thus, it is essential to further understand the behavior of more knowledge of monomers with acrylate and (meth) acrylate unit in supercritical gases (Choi et al., 2016; Jang et al., 2015). Although few works have investigated the phase behavior of methacrylate-based polymers, the high-cost of fluorine-based monomers and their poor solubility have limited their application in various industries (Ritz and P. L. atalova, J. Kriz, J. Genzer, P. Vlcek, 2008; Mohammed et al., 2016; John et al., 2016; Kim et al., 2017).

There are many different approaches were reported for the green synthesis of chemicals (Wang et al., 2022; Meng et al., 2022; Wei et al., 2023), however the utilization of supercritical fluids technique is considered as economical and eco-friendly. The supercritical fluids (SCFs) techniques along with carbon dioxide (CO₂) could be a better substitute in terms of several globally dangerous organic solvents presently applied in the engineering industry due to supercritical carbon dioxide (SC-CO₂) is comparatively cheap, nonflammable, and non-toxic (Goetheer et al., 1999). However, polymers exhibit the inadequate miscibility in solvents, most polymers are miscible in SCFs. At various pressure (p), temperature (T) and concentration, the miscibility of polymer in SC-CO₂ exposes the extraordinary disparity. Being ecologically benign solvent, SC-CO₂ is non-flammable, nontoxic, cheap solvent and also a by-product mass-produced in commercial processes such as hydrogen, ammonia, and ethanol plants (Cooper and Holmes, 1999; Carlota et al., 2007). Also, it has characteristics properties like zero dipole moment, low dielectric constant, quadrupole moment, easily attainable critical point with $T_c = 304.2K$ and $p_c = 7.38MPa$ etc. The two-component system containing SC-CO₂ has various practical functions and hence, to have information of phase equilibria of these mixtures is indispensable. So, the SCFs methodology been utilized to numerous industrial practices trade with various polymer such as anti-solvent precipitation, fine particles creation and polymerization (McHugh and Krukoni, 1994; Cooper, 2000; Tomasko et al., 2003). The lab-made examinations have been constantly published by Byun and their team people. They were discussed the thermodynamic properties of polymers phase behavior study under different supercritical fluids, such as carbon dioxide, ethylene, etc. (Ghoderao et al., 168 (2022); Byun, 2021; Dhamodharan et al., 110 (2022); Dhamodharan, 2022). McHugh and their group also reported various polymers thermodynamic properties under supercritical fluids, they were discussed experimental as well as computational analysis (Mallepally et al., 2016; Wu et al., 2014). Radosz's team performed numerous research works to analyze the phase behavior properties of polymers under supercritical fluids (Albrecht et al., 1996; Folie et al., 1996), and Kiran's team (Kiran, 2016).

In this work, we performed laboratory investigations on the phase equilibria for the PFOA + SC-CO₂ and PFOMA + SC-CO₂ mixtures at maximum pressures and elevated temperatures of approximately 16.84 MPa and 393.2 K, respectively. Our key fact of this research work is to analyze the thermodynamic properties (critical point, dew point, and bubble point) of the discussed two component models

(PFOA + SC-CO₂ and PFOMA + SC-CO₂). The machinery performed in this experiment is a static type by synthetic view technique. The three-phases in presentation of these mixtures was not considered as it is beyond the scope of this work. The data of lab-made trails are correlated by utilizing the Peng Robinson equation of state (PR EOS) under van der Waals single fluid mixing rule (vdW1). The calculation results revealed that laboratory data and the estimated data of the two models were consistent. In addition, there is no other previous studies has been reported for the said system and based on the literature report, this is the first time we have performed the phase behavior examination of a binary model comprising of PFOA + SC-CO₂ and PFOMA + SC-CO₂ mixture.

2. Laboratory investigational section

2.1. Materials

1H, 1H-Perfluorooctyl acrylate (purity > 0.970; CAS 307-98-2) and 1H, 1H-Perfluorooctyl methacrylate (purity > 0.970; CAS 3934-23-4) were obtained from Alfa Aesar Company. Carbon dioxide (purity > 0.999) was purchased from Deok Yang Company. All the materials were utilized as obtained in this research work. The complete details of the utilized materials related to this study is presented in the Table 1. The schematic illustration of the investigated chemicals is presented in Fig. 1.

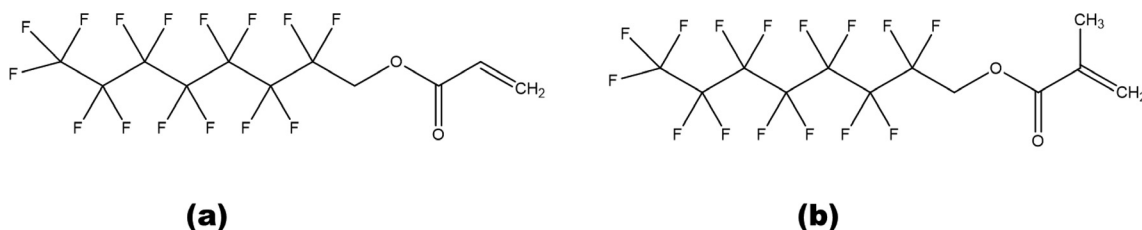
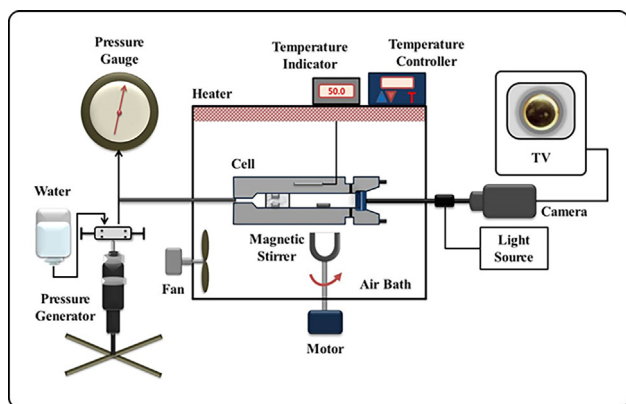
2.2. Device setup and working process

The equipment operated to analyze the phase behavior of two different monomers under SC-CO₂ were performed same as our previous works (Dhamodharan et al., 2022; Kwon et al., 2022; Ghoderao et al., 2022; Ghoderao et al., 2022; Choo et al., 2019). The essential component of the equipment consists of a variable-volume view (3 V) cell, and high-pressure (HP) generator. A thick and strong glass window is associated with the front of the 3 V cell to observe the phase changes. Normally, the thawed (liquid) monomers was passed through the cell roughly ± 0.002 g by the assist of a syringe; then the bare cell is cleansed by numerous trails with N₂ gas to eliminate pinches of organic matters and unwanted air particles. Afterward, CO₂ supplied to the operating 3 V cell roughly ± 0.004 g by the use of a HP bomb. Then the blend inside the 3 V cell compressed to the necessitous pressure by the assist of a wheel type piston.

The 3 V cell pressure was valued with a Heise gauge (having a highest pressure of 34.0 MPa, model CM-53920, made by

Table 1 Specifications of the chemical used in this work.

Chemical name	Mass fraction purity	Molecular formula	Source	CAS RN
Carbon Dioxide	> 0.999	CO ₂	Deok Yang Co.	124-38-9
1H, 1H-Perfluorooctyl Acrylate	> 0.970	C ₁₁ H ₅ F ₁₅ O ₂	Alfa Aesar Co. (GC)	307-98-2
1H, 1H-Perfluorooctyl Methacrylate	> 0.970	C ₁₂ H ₇ F ₁₅ O ₂	Alfa Aesar Co.	3934-23-4

**Fig. 1** Chemical structure of (a) 1H, 1H-perfluorooctyl acrylate and (b) 1H, 1H-perfluorooctyl methacrylate.**Fig. 2** The detailed pictorial representation of experimental apparatus utilized in this research work (McHugh and Krukonic, 1994).

Dresser Ind.) precise to ± 0.02 MPa. A digital meter (accurate to ± 0.005 %, model 7563, made by Yokogawa), was utilized to monitor the 3 V cell temperature and the maintained temperature was less than ± 0.2 K. A borescope (made by Olympus Corp) built-in with a camera is enclosed side to the glass window to observe phase changes via computer. The light dif-

fusion in the 3 V cell was sustained by a fiberoptic wire associated to an elevated-density illuminator and the borescope. The monomers inside the 3 V cell were robustly blended by the support of a magnetic stirrer, which is operated by an external unit. Firstly, the monomer content compressed to a homogeneous phase at steady temperature. The homogeneous phase inside the cell continued at the desired temperature for more than half an hour to accomplish phase equilibrium. Then, the 3 V cell pressure was slightly abridged till a two phases attains. The bubble and dew points were measured, while the first vapor bubble forms and while the earliest teeny mist observed inside the 3 V cell. By changing the pressure and temperature till the critical opalescence, the critical points are marked. The sketch demonstration of the equipment was presented in the Fig. 2.

3. Results analysis

3.1. Experimentation

The laboratory trial data of the PFOA + S_C -CO₂ and PFOMA + S_C -CO₂ systems were investigated, and the experiment was replicated using the HP equipment at a temperature (T), pressure (p), and mole fraction (x) of 0.2 K, 0.02 MPa, and

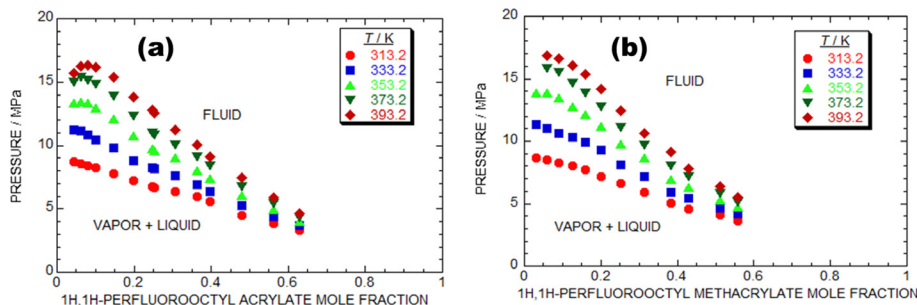
**Fig. 3** The laboratory experimental results of pressure-composition isotherm for as-proposed binary models. (a) \times 1H, 1H-perfluorooctyl acrylate + (1- x) S_C -CO₂ model at various temperatures such as \bullet , 313.2.K; \blacksquare , 333.2.K; \blacktriangle , 353.2.K; \blacktriangledown , 373.2.K; \blacklozenge , 393.2.K. (b) \times 1H, 1H-perfluorooctyl methacrylate + (1- x) S_C -CO₂ model at various temperatures such as \bullet , 313.2 K; \blacksquare , 333.2 K; \blacktriangle , 353.2 K; \blacktriangledown , 373.2 K; \blacklozenge , 393.2 K.

Table 2 Experimental data for the (1H, 1H-perfluorooctyl acrylate + S_C -CO₂) { x C₁₁H₅F₁₅O₂ + (1 - x) S_C -CO₂} system in this work. BP is bubble-point, CP is critical-point and DP is dew-point.

1H, 1H-Perfluorooctyl Acrylate Mole Fraction	p^a / MPa	Transition ^b
T^a / K = 313.2		
0.044	8.72	BP
0.063	8.59	BP
0.081	8.42	BP
0.101	8.24	BP
0.147	7.80	BP
0.198	7.20	BP
0.249	6.74	BP
0.253	6.68	BP
0.307	6.35	BP
0.363	5.97	BP
0.396	5.55	BP
0.478	4.48	BP
0.563	3.83	BP
0.630	3.31	BP
T / K = 333.2		
0.044	11.22	BP
0.063	11.15	BP
0.081	10.83	BP
0.101	10.45	BP
0.147	9.80	BP
0.198	8.79	BP
0.249	8.22	BP
0.253	8.20	BP
0.307	7.59	BP
0.363	6.93	BP
0.396	6.38	BP
0.478	5.24	BP
0.563	4.41	BP
0.630	3.72	BP
T / K = 353.2		
0.044	13.35	DP
0.063	13.43	CP
0.081	13.32	BP
0.101	12.93	BP
0.147	12.10	BP
0.198	10.72	BP
0.249	9.74	BP
0.253	9.61	BP
0.307	8.99	BP
0.363	8.04	BP
0.396	7.35	BP
0.478	6.06	BP
0.563	4.96	BP
0.630	4.00	BP
T / K = 373.2		
0.044	15.00	DP
0.063	15.37	DP
0.081	15.11	BP
0.101	14.79	BP
0.147	13.86	BP
0.198	12.31	BP
0.249	10.95	BP
0.253	10.79	BP
0.307	10.04	BP

Table 2 (continued)

1H, 1H-Perfluorooctyl Acrylate Mole Fraction	p^a / MPa	Transition ^b
0.363	9.07	BP
0.396	8.38	BP
0.478	6.79	BP
0.563	5.41	BP
0.630	4.35	BP
T / K = 393.2		
0.044	15.70	DP
0.063	16.25	DP
0.081	16.36	CP
0.101	16.17	BP
0.147	15.41	BP
0.198	13.83	BP
0.249	12.76	BP
0.253	12.55	BP
0.307	11.21	BP
0.363	10.03	BP
0.396	9.14	BP
0.478	7.45	BP
0.563	5.85	BP
0.630	4.62	BP

^a Standard uncertainties are $u(T) = 0.12$ K, $u(p) = 0.2$ MPa and $u(x) = 0.0008$.

^b BP: Bubble-point, CP: Critical-point, DP: Dew-point.

0.002, respectively. The solubility isotherms of the PFOA + S_C -CO₂ and PFOMA + S_C -CO₂ systems with a change in temperatures from 313.2 K to 393.2 K were constructed depending on the outcomes with two sovereign factors with an estimated error of less than $\pm 0.1\%$.

The lab-based trail data of p , composition (x) isotherms at various temperatures, such as 313.2 K to 393.2 K and several pressures raise from 3.31 to 16.84 MPa for the PFOA + S_C -CO₂ system. Fig. 3a and Table 2 shows the lab-based trail data of PFOA + S_C -CO₂ system. The Fig. 3a, exposes that, described BP pressure rises with the rise in temperature which is attributes of type-I phase behavior (Byun, 2017; Lee et al., 2018). As shown in Fig. 3a, the critical p of the PFOA + S_C -CO₂ system is rising in regard to the increasing temperature, that is the early critical pressure was noted at 13.43 MPa in regard to 353.2 K, then the elevated pressure value of 16.36 MPa was accomplished at 393.2 K, which evidence that the critical point (CP) of the PFOA + S_C -CO₂ system rises with respect to raising T .

Similarly, the PFOMA + S_C -CO₂ model was also carried out with the various temperatures and difference pressures same as PFOA + S_C -CO₂ model. The studied lab-based investigational data of the PFOMA + S_C -CO₂ system is presented in the Fig. 3b and Table 3. The Fig. 3a, exposes that, described BP pressure rises with the rise in temperature which is attributes of type-I BP (Byun, 2017; Lee et al., 2018). In addition, there was a notable decrease in the solubility of the monomer in CO₂ with increase T at a fixed pressure range. Nevertheless, as shown in Fig. 3 (a-b), both two-component models demonstrate type-I model and possibly there were no three phases achieved at various operated temperatures in both the models.

Table 3 Experimental data for the (1H, 1H-perfluorooctyl methacrylate + SC-CO₂) {*x* C₁₂H₇F₁₅O₂ + (1 - *x*) SC-CO₂} system in this work. BP is bubble-point, CP is critical-point and DP is dew-point.

1H, 1H-Perfluorooctyl Methacrylate Mole Fraction	p^a / MPa	Transition ^b
T^a / K = 313.2		
0.032	8.67	BP
0.059	8.49	BP
0.091	8.24	BP
0.125	8.04	BP
0.159	7.70	BP
0.200	7.18	BP
0.252	6.59	BP
0.315	5.90	BP
0.382	5.04	BP
0.430	4.59	BP
0.513	4.07	BP
0.557	3.66	BP
T / K = 333.2		
0.032	11.38	BP
0.059	11.05	BP
0.091	10.66	BP
0.125	10.31	BP
0.159	9.90	BP
0.200	9.29	BP
0.252	8.14	BP
0.315	7.14	BP
0.382	5.93	BP
0.430	5.41	BP
0.513	4.69	BP
0.557	4.21	BP
T / K = 353.2		
0.032	13.84	DP
0.059	13.87	CP
0.091	13.48	BP
0.125	12.72	BP
0.159	12.10	BP
0.200	11.17	BP
0.252	9.79	BP
0.315	8.66	BP
0.382	6.90	BP
0.430	6.31	BP
0.513	5.31	BP
0.557	4.76	BP
T / K = 373.2		
0.059	15.83	BP
0.091	15.49	BP
0.125	14.66	BP
0.159	13.90	BP
0.200	12.76	BP
0.252	11.14	BP
0.315	9.69	BP
0.382	8.00	BP
0.430	7.21	BP
0.513	5.86	BP
0.557	5.10	BP
T / K = 393.2		
0.059	16.84	BP
0.091	16.60	BP

Table 3 (continued)

1H, 1H-Perfluorooctyl Methacrylate Mole Fraction	p^a / MPa	Transition ^b
0.125	16.04	BP
0.159	15.35	BP
0.200	14.21	BP
0.252	12.48	BP
0.315	10.66	BP
0.382	9.14	BP
0.430	7.83	BP
0.513	6.41	BP
0.557	5.55	BP

^a Standard uncertainties are $u(T) = 0.12$ K, $u(p) = 0.2$ MPa and $u(x) = 0.0008$.

^b BP: Bubble-point, CP: Critical-point, DP: Dew-point.

3.2. Computational analysis

The *PR EOS* model was utilized for comparison with the obtained laboratory trail values such as the BP, dew point (DP), and CP of the isothermal phase behavior, and the formulas used are expressed below:

$$P = \frac{RT}{v-b} - \frac{a(T)}{v(v+b) + b(v-b)} \quad (1)$$

$$a(T) = 0.45724 \frac{R^2 T_c^2}{P_c} \alpha(T_r, \omega) \quad (2)$$

$$b(T_c) = 0.07780 \frac{RT_c}{P_c} \quad (3)$$

$$\alpha(T_r, \omega) = \left(1 + \kappa \left(1 - T_r^{\frac{1}{2}}\right)\right)^2 \quad (4)$$

where, κ can be expressed as,

$$\kappa = 0.37464 + 1.5422\omega - 0.26999 \quad (5)$$

The vdW1 rules are expressed below,

$$a_{mix} = \sum_i \sum_j x_i x_j a_{ij} \quad (6)$$

$$b_{mix} = \sum_i \sum_j x_i x_j b_{ij} \quad (7)$$

$$a_{ij} = (a_{ii} a_{jj})^{\frac{1}{2}} (1 - \kappa_{ij}) \quad (8)$$

$$b_{ij} = \frac{1}{2} (b_{ii} + b_{jj}) (1 - \eta_{ij}) \quad (9)$$

where the interaction parameters “ η_{ij} ” and “ κ_{ij} ” were calculated by reducing the objective function (OF) expressed in eq. (10) at a base T of 353.2 K. In addition, the root means square deviation (*RMSD*) and *OF* are calculated using the formulas below:

$$OF = \sum_i^N \left(\frac{P_{exp} - P_{cal}}{P_{exp}} \right)^2 \quad (10)$$

Table 4 The properties of pure component in carbon dioxide, 1H, 1H-perfluorooctyl acrylate and 1H, 1H-perfluorooctyl methacrylate.

Compounds	M_w	T_b / K	T_c / K	p_c / MPa	ω
Carbon Dioxide	44.01		304.2	7.38	0.225
1H, 1H-Perfluorooctyl Acrylate	454.13	481.6 ^a	614.7	1.28	0.708
1H, 1H-Perfluorooctyl Methacrylate	468.16	493.0 ^b	625.6	1.20	0.710

^a : Calculated value ^b: Guidechem.

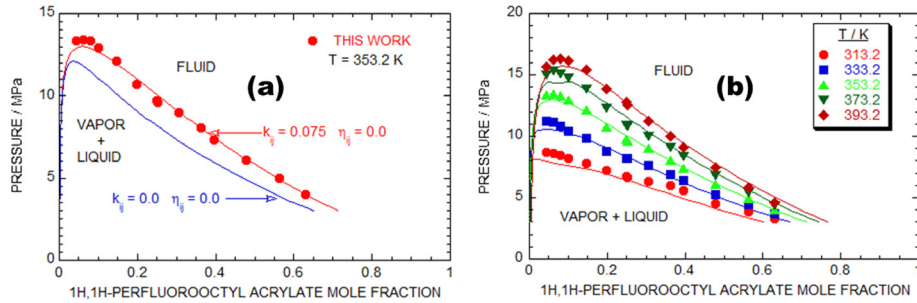


Fig. 4 The comparative study analysis of experimental and *PR EOS* simulated results of as-proposed binary mixtures models. (a) Plot of pressure against mole fraction to illustrate the comparison of experimental data (symbols) for the (1H, 1H-perfluorooctyl acrylate + S_C - CO_2) $\{(1-x) S_C$ - CO_2 + x ($C_{11}H_5F_{15}O_2$) $\}$ model with calculations obtained from the *PR EOS* by κ_{ij} and η_{ij} set equal to zero (dashed lines), and κ_{ij} equal to 0.075 and η_{ij} equal to 0.0 (solid lines) at $T=353.2$ K. (b) 1H, 1H-perfluorooctyl acrylate + S_C - CO_2 $\{(1-x) S_C$ - CO_2 + x ($C_{11}H_5F_{15}O_2$) $\}$.

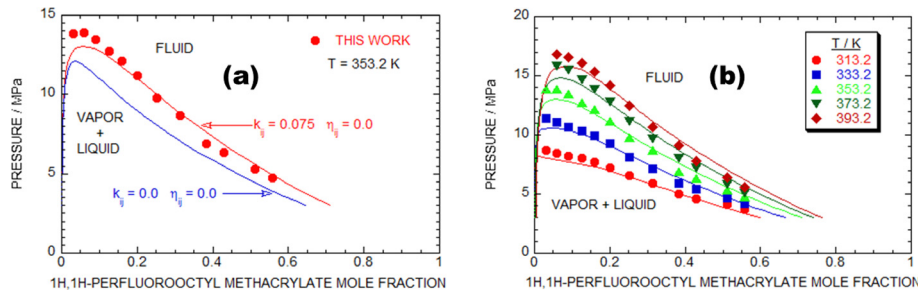


Fig. 5 The comparative study analysis of experimental and *PR EOS* simulated results of as-proposed binary mixtures models. (a) Plot of pressure against mole fraction to illustrate the comparison of experimental data (symbols) for the (1H, 1H-perfluorooctyl methacrylate + S_C - CO_2) $\{(1-x) S_C$ - CO_2 + x ($C_{12}H_7F_{15}O_2$) $\}$ model with calculations obtained from the *PR EOS* by κ_{ij} and η_{ij} set equal to zero (dashed lines), and κ_{ij} equal to 0.075 and η_{ij} equal to 0.0 (solid lines) at $T=353.2$ K. (b) 1H, 1H-perfluorooctyl methacrylate + S_C - CO_2 $\{(1-x) S_C$ - CO_2 + x ($C_{12}H_7F_{15}O_2$) $\}$.

$$RMSD(\%) = \sqrt{\frac{OF}{N}} 100 \quad (11)$$

where “N” in equations (10) and (11) denotes the data points counts, and we have optimized the OF with the help of Marquardt algorithm (Kuester and Mize, 1973). The p_c , ω , and T_c of the neat PFOA, PFOMA, and CO_2 were evaluated using the *PR EOS*, and the investigated information is listed in Table 4. The critical characters of the PFOA, and PFOMA were assessed using the Joback and Lydersen’s method (Peng and Robinson, 1976; Poling et al., 2001). The vapor pressure assessment was performed using the Lee-Kesler technique (Peng and Robinson, 1976; Poling et al., 2001).

Fig. 4a shows the comparison of the laboratory trail and *PR EOS* assessed values of the PFOA + S_C - CO_2 system at $T = 353.2$ K. The red dots indicate the laboratory trail data counts, and the red mark displays a good fit of computational analysis data obtained by the aid of *PR EOS*. The blue marks imply outcomes obtained using $k_{ij} = 0.0, \eta_{ij} = 0.0$, whereas the red mark indicate outcomes obtained using the matched k_{ij} and η_{ij} . The independent interaction parameter of the *PR EOS* exposes good match with the laboratory trail data at 353.2 K. The *PR EOS*, adjusted value for PFOA + S_C - CO_2 system are $\eta_{ij} = 0.0, k_{ij} = 0.075$ at 353.2 K.

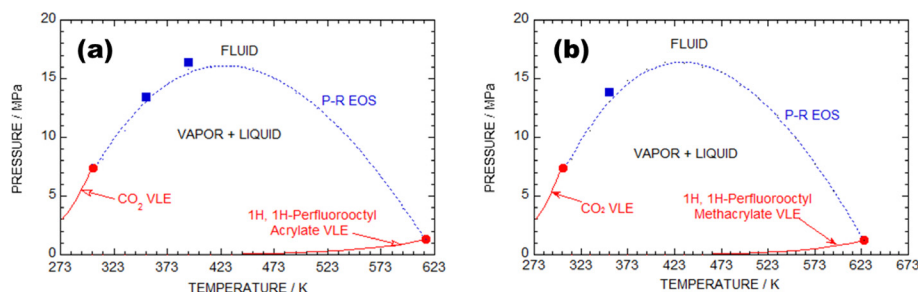


Fig. 6 Plot of pressure against temperature for the as-proposed binary models. (a) 1H, 1H-perfluorooctyl acrylate + $S_C\text{-CO}_2$ model. The solid lines and the solid circles represent the (vapor + liquid) lines and the critical points for pure CO_2 and 1H, 1H-perfluorooctyl acrylate. The solid squares are critical points determined from isotherms measured in this work. (b) 1H, 1H-perfluorooctyl methacrylate + $S_C\text{-CO}_2$ model. The solid lines and the solid circles represent the (vapor + liquid) lines and the critical points for pure CO_2 and 1H, 1H-perfluorooctyl methacrylate. The solid squares are critical points determined from isotherms measured in this work.

Fig. 4b, demonstrating the competitive discussion of lab-made trail and computational analysis data of the p - x isotherms at various temperatures (313.2 to 393.2) K for the PFOA + $S_C\text{-CO}_2$ system engaged using the adjusted data of the sovereign factors of k_{ij} and η_{ij} calculated at $T = 353.2$ K. In agreement with the **Fig. 4b**, the lab-based investigational results, and the PR EOS adjusted data of the PFOA + $S_C\text{-CO}_2$ system shows a decent agreement. The $RMSD$ (%) of all the laboratory trial T was 5.08 % for 70 data counts.

Fig. 5a shows a comparative study analysis of laboratory trail and simulated p - x isotherms for the PFOMA + $S_C\text{-CO}_2$ system at $T = 353.2$ K. The red dots denote to lab-based investigational results, and the red line indicates that the laboratory results were well matched with the simulated values obtained using PR EOS. The blue mark indicates the outcomes obtained using $k_{ij} = 0.0, \eta_{ij} = 0.0$ whereas the red marks represent the outcomes obtained using the matched k_{ij} and η_{ij} . The two component interaction elements of the PR EOS model were in good agreement with the laboratory trail data at 353.2 K. The PR EOS adjusted data for PFOMA + $S_C\text{-CO}_2$ system at $T = 353.2$ K were $\eta_{ij} = 0.0, k_{ij} = 0.075$.

Fig. 5b displays that the comparative discussion of laboratory trail response and computational p - x isotherms at various temperatures from 313.2 K to 393.2 K for the PFOMA + $S_C\text{-CO}_2$ system engaged the adjusted data of the sovereign factors of k_{ij} and η_{ij} lofted at $T = 353.2$ K. The image revealed that the obtained laboratory trail results and the PR EOS optimized data of the PFOMA + $S_C\text{-CO}_2$ system were well matched. The $RMSD$ (%) of all the investigated T was 5.36 % for 58 data counts.

Fig. 6a shows the PR EOS predicted critical curve (CC) for the PFOA + $S_C\text{-CO}_2$ system. The red marks in **Fig. 6a** indicate the vapor p of the pure PFOA and CO_2 , which was assessed using the Lee-Kesler approach (Peng and Robinson, 1976; Poling et al., 2001). The red dots emphasize the CP of the pure CO_2 and PFOA. The area above the blue mark indicated that the system is in one phase (fluid), and the area below indicates two phases (vapor and liquid). The blue dashed lines represent the information obtained from the PR EOS for the PFOA + $S_C\text{-CO}_2$ model at $T = 353.2$ K.

Fig. 6b shows the PR EOS estimated CC for the PFOMA + $S_C\text{-CO}_2$ system. The red lines in **Fig. 6b** correspond to the vapor p of the pure PFOMA and CO_2 ,

which was assessed by the help of Lee-Kesler approach (Peng and Robinson, 1976; Poling et al., 2001). The red dots indicate the CP of the pure CO_2 and PFOMA. In **Fig. 6b**, the area above the blue marking represents one phase (fluid), and the below the mark represents two phases (vapor-liquid). The consequential CCs expose type-I system. The blue marking relates to the estimated data accomplished through PR EOS of the PFOMA + $S_C\text{-CO}_2$ system at $T = 353.2$ K. Moreover, the examined CCs of the as-proposed two-component models were consistent with the laboratory trail data and computational response, which was obtained using PR EOS with two alterable parameters.

4. Conclusions

In this study, high-pressure laboratory-obtained trial data of the (p, x) isotherm for the (PFOA + $S_C\text{-CO}_2$ and PFOMA + $S_C\text{-CO}_2$) two-component models assessed using a synthetic approach equipment (3 V cell) at various temperatures from 313.2 to 393.2 K and a maximum p of ~ 24 MPa were obtained. Both (PFOA + $S_C\text{-CO}_2$ and PFOMA + $S_C\text{-CO}_2$) systems did not exhibit three phases (liquid + liquid + vapor) at any operated temperatures. The PR EOS predicted the phase behavior for the (PFOA + $S_C\text{-CO}_2$, and PFOMA + $S_C\text{-CO}_2$) systems using two temperature sovereign mixture synergy factors. The critical curves between the simulated and laboratory-obtained trail data were consistent base on the two-adjustable parameters of the PR EOS. The $RMSD$ (%) for the PFOA + $S_C\text{-CO}_2$ [$k_{ij} = 0.075, \eta_{ij} = 0.0$], and PFOMA + $S_C\text{-CO}_2$ [$k_{ij} = 0.075, \eta_{ij} = 0.0$] models using two factors determined at 353.2 K evaluated using the alterable parameters at each T were 5.08 %, and 5.36 %, respectively.

CRedit authorship contribution statement

Duraisami Dhamodharan: Investigation, Writing – original draft. **Min-Soo Park:** Experimental Assistant, Simulation. **Suhail Mubarak:** Experimental Assistant, Simulation. **Hun-Soo Byun:** Conceptualization, Visualization, Supervision, Project administration, Writing – review & editing.

Declaration of Competing Interest

The authors declare that they have no known competing financial interests or personal relationships that could have appeared to influence the work reported in this paper.

Acknowledgements

This work was supported by the National Research Foundation of Korea (NRF) grant funded by the Korea government (MSIT) (No. 2021R1A2C2006888).

References

- Albrecht, K.L., Stein, F.P., Han, S.J., Gregg, C.J., Radosz, M., 1996. Phase equilibria of saturated and unsaturated polyisoprene in sub- and supercritical ethane, ethylene, propane, propylene, and dimethyl ether. *Fluid Phase Equilib.* 117, 84–91. [https://doi.org/10.1016/0378-3812\(95\)02940-0](https://doi.org/10.1016/0378-3812(95)02940-0).
- Byun, H.S., 2017. High pressure phase equilibria for the mixture of CO₂ + 3-phenyl propionitrile and CO₂ + 2-phenyl butyronitrile systems. *J. Supercrit. Fluids* 120, 218–225. <https://doi.org/10.1016/j.supflu.2016.05.045>.
- Byun, H.-S., 2021. Phase separation of two- and three-component solution for the poly (pentyl acrylate-co-methyl methacrylate) + compressed solvents and copolymer preparation by supercritical dispersion polymerization. *J. Ind. Eng. Chem.* 99, 158–171. <https://doi.org/10.1016/j.jiec.2021.04.018>.
- Carlot, V.D.M., Soares da Silva, M., Casimiro, T., Cabrita, E.J., Aguiar-Ricardo, A., 2007. Boron trifluoride catalyzed polymerization of 2-substituted-2-oxazolones in supercritical carbon dioxide. *Green Chem.* 9, 948–953. <https://doi.org/10.1039/B617940A>.
- Choi, Y.-S., Chio, S.-W., Byun, H.-S., 2016. Phase behavior for the poly(alkyl methacrylate) + supercritical CO₂ + DME mixture at high pressures. *Kor. J. Chem. Eng.* 33, 277–284. <https://doi.org/10.1007/s11814-015-0208-6>.
- Choo, Y.S., Yeo, W.H., Byun, H.S., 2019. Phase equilibria and cloud-point behavior for the poly (2-phenylethyl methacrylate) in supercritical CO₂ with monomers as co-solvent. *J. CO₂ Utilization* 31, 215–225. <https://doi.org/10.1016/j.jcou.2019.03.008>.
- Cooper, A.I., 2000. Polymer synthesis and processing using supercritical carbon dioxide. *J. Mater. Chem.* 10, 207–234. <https://doi.org/10.1039/A906486I>.
- Cooper, A.I., Holmes, A.B., 1999. Synthesis of molded monolithic porous polymers using supercritical carbon dioxide as the porogenic solvent. *Adv. Mater.* 11, 1270–1274. [https://doi.org/10.1002/\(SICI\)1521-4095\(199910\)11:15 < 1270::AID-ADMA1270 > 3.0.CO;2-E](https://doi.org/10.1002/(SICI)1521-4095(199910)11:15 < 1270::AID-ADMA1270 > 3.0.CO;2-E).
- Dhamodharan, D., 2022. Pradnya Prabhakar Ghoderao, Hun-Soo Byun, Binary Equilibrium Behavior for the N, N-Dimethylaniline and N, N-diethylaniline in Supercritical Carbon Dioxide. *J. Mol. Liq.* 357. <https://doi.org/10.1016/j.molliq.2022.119112> 119112.
- D Dhamodharan, Pradnya NP Ghoderao, Cheol-Woong Park, Hun-Soo Byun. Experimental and computational investigation of two-component mixtures for the alkyl (ethyl, propyl and butyl) oleate in supercritical carbon dioxide. *J. Ind. Eng. Chem.*, 110 (2022) 367–374. [10.1016/j.jiec.2022.03.013](https://doi.org/10.1016/j.jiec.2022.03.013).
- Dhamodharan, D., Ghoderao, P.N.P., Park, C.-W., Byun, H.-S., 2022. Bubble and Dew- Point Measurement of Mixture for the 1H,1H,2H-Perfluoro-1-octene and 1H,1H,2H,2H- Perfluoro-1-octanol in Supercritical CO₂. *New J. Chem.* 46, 7271–7278. <https://doi.org/10.1039/D2NJ00670G>.
- Folie, B., Gregg, C., Luft, G., Radosz, M., 1996. Phase equilibria of poly (ethylene-co-vinyl acetate) copolymers in subcritical and supercritical ethylene and ethylene vinyl acetate mixtures. *Fluid Phase Equilib.* 120, 11–37. [https://doi.org/10.1016/0378-3812\(95\)02981-8](https://doi.org/10.1016/0378-3812(95)02981-8).
- Ghoderao, P.N.P., Dhamodharan, D., Byun, H.-S., 2022. Co-solvent concentration impact on the cloud point behavior of 2- and 3-ingredient systems of the poly (tridecyl methacrylate) in supercritical CO₂. *New J. Chem.* 46, 2300–2308. <https://doi.org/10.1039/D1NJ05607G>.
- Ghoderao, P.N.P., Dhamodharan, D., Mubarak, S., Byun, H.-S., 2022. Phase behavioral study of binary systems for the vinyl benzoate, vinyl pivalate and vinyl octanoate with carbon dioxide at high-pressure. *J. Mol. Liq.* 358, 119131.
- P.N.P. Ghoderao, D. Dhamodharan, and H.-S. Byun. Binary Mixture Phase Equilibria for the Vinyl Laurate, Vinyl Methacrylate and Vinyl Propionate under High Pressure Carbon Dioxide. *The J. Chem. Thermodyn.*, 168 (2022) 106746.
- Goetheer, E.L.V., Vorstman, M.A.G., Keurentjes, J.T.F., 1999. Opportunities for process intensification using reverse micelles in liquid and supercritical carbon dioxide. *Chem. Eng. Sci.* 54, 1589–1596. [https://doi.org/10.1016/S0009-2509\(99\)00043-3](https://doi.org/10.1016/S0009-2509(99)00043-3).
- Jang, Y.-S., Choi, Y.S., Byun, H.-S., 2015. Phase behavior for the poly (2-methoxyethyl acrylate) + supercritical solvent + cosolvent mixture and CO₂ + 2-methoxyethyl acrylate system at high pressure. *Kor. J. Chem. Eng.* 32, 958–966. <https://doi.org/10.1007/s11814-014-0316-8>.
- John, L., Janeta, M., Rajczakowska, M., Ejfler, J., Lydzba, D., Szafert, S., 2016. Synthesis and microstructural properties of the scaffold based on a 3-(trimethoxysilyl) propyl methacrylate-POSS hybrid towards potential tissue engineering applications. *RSC Adv.* 6, 66037–66047. <https://doi.org/10.1039/C6RA10364B>.
- Kim, S.Y., Wee, J.-H., Yang, C.-M., Kim, B.-H., 2017. Electrochemical capacitor performance of 2-(trimethylsilyloxy) ethyl methacrylate-derived highly mesoporous carbon nanofiber composite containing MnO₂. *J. Electroanal. Chem.* 801, 403–409. <https://doi.org/10.1016/j.jelechem.2017.07.028>.
- Kiran, E., 2016. Supercritical fluids and polymers-The year in review-2014. *J. Supercrit. Fluids* 110, 126–153. <https://doi.org/10.1016/j.supflu.2015.11.011>.
- Kirk-Othmer, Encyclopedia of Chemical Technology, John Wiley & Sons, New York, 1981
- Kuester, J.L., Mize, J.H., 1973. *Optimization Techniques with Fortran*. McGraw-Hill, New York.
- Kwon, Y.-T., Dhamodharan, D., Choi, H., Shim, S.-W., Byun, H.-S., 2022. Phase equilibrium study of binary systems for the PGME + CO₂ and PGMEA + CO₂ mixture at high pressure by experimentally and computationally. *Kor. J. Chem. Eng.* 39, 2783–2791. <https://doi.org/10.1007/s11814-022-1110-7>.
- Lee, B.S., Lee, J.K., Bong, J.H., Byun, H.S., 2018. Phase behavior for the 2-(trimethylsilyloxy) ethyl methacrylate and 3-(trimethoxysilyl) propyl methacrylate in supercritical carbon dioxide. *Fluid Phase Equilib.* 462, 1–5. <https://doi.org/10.1016/j.fluid.2018.01.013>.
- Mallepally, R.R., Gadepalli, V.S., Bamgbade, B.A., Cain, N., McHugh, M.A., 2016. Phase behavior and densities of propylene + hexane binary mixtures to 585 K and 70 MPa. *J. Chem. Eng. Data* 61, 2818–2827. <https://doi.org/10.1021/acs.jced.6b00181>.
- McHugh, M., Krukoni, V., 1994. *Supercritical Fluid Extraction: Principles and Practice 2nd*. Butterworth-Heinemann, Boston.
- Meng, G., Jin, M., Wei, T., Liu, Q., Zhang, S., Peng, X., Luo, J., Liu, X., 2022. MoC nanocrystals confined in N-doped carbon nanosheets toward highly selective electrocatalytic nitric oxide reduction to ammonia. *Nano Res.* 15, 8890–8896. <https://doi.org/10.1007/s12274-022-4747-y>.
- A.H. Mohammed, M.B. Ahmad, N.A. Ibrahim, N. Zainuddin, Synthesis and monomer reactivity ratios of acrylamide with 3-(trimethoxysilyl) propyl methacrylate and tris (methoxyethoxy) vinylsilane copolymers. *Polimery*, 61 (11-12) (2016) 758–765.
- Peng, D.Y., Robinson, D.B., 1976. A new two-constant equation of state. *Ind. Eng. Chem. Fundamen.* 15, 59–64. <https://doi.org/10.1021/i160057a011>.
- B.E. Poling, J.M. Prausnitz, and J.P. O'Connell. Properties of gases and liquids. McGraw-Hill Education. 2001
- P. Ritz, P. Latalova, J. Kriz, J. Genzer, P. Vlcek, Statistical copolymers of 2-(trimethylsilyloxy) ethyl methacrylate and methyl methacrylate synthesized by ATRP. *J. Polym. Sci., Part A: Polym. Chem.*, 46 (2008) 1919–1923.

- Tomasko, D.L., Li, H., Liu, D., Han, X., Wingert, M.J., Lee, L.J., Koelling, K.W., 2003. A review of CO₂ applications in the processing of polymers. *Ind. Eng. Chem. Res.* 42, 6431–6456. <https://doi.org/10.1021/ie030199z>.
- Wang, X., Liu, S., Zhang, H., Zhang, S., Meng, G., Liu, Q., Sun, Z., Luo, J., Liu, X., 2022. Polycrystalline S_nS_x nanofilm enables CO₂ electroreduction to formate with high current density. *Chem. Commun.* 58, 7654–7657. <https://doi.org/10.1039/D2CC01888H>.
- Wei, T., Liu, W., Zhang, S., Liu, Q., Luo, J., Liu, X., 2023. A dual-functional Bi-doped Co₃O₄ nanosheet array towards high efficiency 5-hydroxymethylfurfural oxidation and hydrogen production. *Chem. Commun.* 59, 442–445. <https://doi.org/10.1039/D2CC05722K>.
- Wu, Y., Newkirk, M.S., Dudek, S.T., Williams, K., Krukoni, V., McHugh, M.A., 2014. Architectural effects on the solution behavior of linear and star polymers in propane at high pressures. *Ind. Eng. Chem. Res.* 53, 10133–10143. <https://doi.org/10.1021/ie5011417>.